Effect of Main Elements (Zn, Mg, and Cu) on Hot Tearing Susceptibility During Direct-Chill Casting of 7xxx Aluminum Alloys

Li, Y.; Zhang, Z. R.; Zhao, Z. Y.; Li, H. X.; Katgerman, L.; Zhang, J. S.; Zhuang, L. Z.

DOI
10.1007/s11661-019-05268-z

Publication date
2019

Document Version
Accepted author manuscript

Published in
Metallurgical and Materials Transactions A: Physical Metallurgy and Materials Science

Citation (APA)
Li, Y., Zhang, Z. R., Zhao, Z. Y., Li, H. X., Katgerman, L., Zhang, J. S., & Zhuang, L. Z. (2019). Effect of Main Elements (Zn, Mg, and Cu) on Hot Tearing Susceptibility During Direct-Chill Casting of 7xxx Aluminum Alloys. *Metallurgical and Materials Transactions A: Physical Metallurgy and Materials Science*, *50*(8), 3603-3616. https://doi.org/10.1007/s11661-019-05268-z

Effect of Main Elements (Zn, Mg, and Cu) on Hot Tearing Susceptibility During Direct-Chill Casting of 7xxx Aluminum Alloys

Y. LI, Z.R. ZHANG, Z.Y. ZHAO, H.X. LI, L. KATGERMAN, J.S. ZHANG, and L.Z. ZHUANG

New 7xxx aluminum alloys with high alloying contents are being designed, which could induce serious hot tearing defects during direct-chill (DC) casting. Among all factors affecting hot tearing of 7xxx alloys, undoubtedly alloying elements play a significant role. In this study, the effect of main alloying elements (Zn, Mg, and Cu) on hot tearing of grain-refined Al-*x*Zn-*y*Mg-*z*Cu alloys was investigated by a dedicated hot tearing rating apparatus simulating the DC-casting process. It was found that the minimum and maximum hot tearing susceptibilities occur for 4 to 6 and 9 wt pct Zn, respectively, indicating the complicated effect of Zn content. The hot tearing resistance of grain-refined Al-9Zn-*y*Mg-*z*Cu alloys is enhanced with increasing Mg content but is deteriorated with increasing Cu content. This can be attributed to the interaction of the thermal stresses, melt feeding, and final eutectics. The observed tendencies of the main alloying elements on hot tearing were also confirmed for four commercial 7xxx alloys. In addition, both the load value at non-equilibrium solidus and the SKK criterion proposed by Suyitno *et al.* using measured load developments were found to be good indicators in predicting hot tearing susceptibility. This study can provide a beneficial guide in designing 7xxx alloys considering the potential occurrence of hot cracks beforehand.

https://doi.org/10.1007/s11661-019-05268-z

I. INTRODUCTION

7XXX aluminum alloys are widely applied in the aircraft industry due to their very high tensile strength and good fracture toughness.[1] Currently, to improve performance such as strength, damage tolerance, and corrosion resistance,[2–6] new 7xxx alloys are being designed with higher alloying contents. To produce these new alloys, large-size direct-chill (DC) casting ingots/billets have to be fabricated. The larger ingots together with the higher alloying contents will most likely induce casting defects during DC casting,[2] and hot tearing is one of the most common defects. It is well known that high casting speeds and large ingot/billet diameters can easily lead to higher hot tearing susceptibilities in 7xxx alloys.[7–9] Besides these factors, alloy composition is another crucial point to affect the hot tearing susceptibility. Bai *et al.*[10,11] investigated the hot tearing and thermal contraction behavior of several commercial 7xxx alloys. It was found that different alloys exhibited different hot tearing resistance. Gildemeister[4] studied the relationship between the hot tearing behavior of two Al-Zn-Mg-Cu alloys (AA7075 and a modified AA7075) and their as-cast microstructures using a small-scale DC caster. It was found that alloying elements affect the quantity, scale, and constitution of the eutectic structures and thus influence hot tearing susceptibility. We recently investigated the hot tearing behavior of non-grain-refined Al-*x*Zn-2Mg-2Cu alloys and found that the minimum and maximum hot tearing susceptibilities were observed at 4 and 12 wt pct Zn contents, respectively. However, grain refiners were not added. Note that grain refinement often decreases the hot tearing susceptibility of 7xxx alloys.[11–13] Eskin *et al.*[14] have reviewed hot tearing in aluminum alloys. They pointed out that indeed the main alloying elements can influence the hot tearing resistance of non-grain-refined 7xxx alloys. Although many efforts have been made, some challenges still exist. For example, the hot tearing susceptibility of non-refined Al-Zn-Mg-Cu model alloys with Zn and Cu contents less than 10 and 1 wt pct, respectively, has been summarized.[14]

Y. LI, Z.R. ZHANG, Z.Y. ZHAO, H.X. LI, J.S. ZHANG, and L.Z. ZHUANG are with the State Key Laboratory for Advanced Metals and Materials, University of Science and Technology Beijing, Beijing, 100083, PR China. Contact e-mails: hongxiang_li@vip.163.com; linzhongzhuang@yahoo.com L. KATGERMAN is with the Department of Materials Science and Engineering, Delft University of Technology, Mekelweg 2, 2628 CD Delft, The Netherlands.

Manuscript submitted February 5, 2019.

However, the composition range of 7xxx alloys is actually much wider[15]: Zn concentrations lie between 2 and 12 wt pct; Cu concentrations are between about 0.5 and 3 wt pct; Mg concentrations range from about 1 to 3 wt pct; grain refiners are often added. Furthermore, the used testing molds do not simulate DC-casting conditions, *i.e.*, the DC ingot experiences different thermomechanical situations during solidification, and thus the obtained results could be quite different from the actual casting practice. Therefore, it is indeed necessary to further investigate the influence of main alloying elements with a wide composition range on hot tearing susceptibility in 7xxx aluminum alloys, especially with grain refiner additions in a setup simulating real DC-casting conditions.

To study the hot tearing behavior, experimental methods combined with hot tearing criteria can be a good approach. Two kinds of experiments are often employed to investigate hot tearing: pilot-scale castings[5,16] and dedicated hot tearing apparatuses.[2,17–23] The pilot-scale casting is the most direct approach to achieve goals. However, it is time-consuming and costly. In contrast, using dedicated hot tearing devices can greatly save time and effort. Tests including ring mold[23] and constrained-rod casting mold[18–20] that simulate shape casting have been used to evaluate various alloy systems. In recent years, these techniques have become more and more sophisticated by being equipped with a load or displacement cell.[17–20] Inspired by the design of a dog-bone-shaped mold,[21] Instone *et al.*[22] developed a hot tearing test rig to measure the hot tearing susceptibility of an alloy and its contraction or load developments. This apparatus simulates DC casting and has been applied to different alloying systems, including relatively pure Al,[22] Al-Cu,[24–26] 3xxx,[26,27] and 6xxx[26,28,29] alloys. We recently also developed a dedicated hot tearing rating apparatus simulating DC-casting conditions.[2] This apparatus is based on the linear contraction apparatus developed by Eskin *et al.*[17] However in our setup, the casting was constrained during solidification when the evolutions of load, temperature, and time were obtained. Here, this experimental apparatus will be applied to systematically reveal the effect of main alloying elements on the hot tearing susceptibility of 7xxx alloys.

Apart from experimental approaches, many non-mechanical and mechanical criteria have been proposed to predict hot tearing.[14,30,31] Suyitno *et al.*[16] have evaluated eight commonly used criteria by implementing them into a thermomechanical model of DC casting. It was found that the RDG criterion[32] could predict the hot tearing susceptibility for all studied process parameters, although it was not able to accurately predict whether hot tears will form during DC casting.[16] To address this problem, Suyitno *et al.*[31] went further and proposed a microporosity-related hot tearing criterion, named SKK criterion (first letters of the authors' name). This criterion calculates the formation of pores during the last stage of solidification from the insufficient feeding in the mushy zone. Whether pores will develop into hot tears depends on the critical size determined by the Griffith model for brittle fracture. The predictions made by the SKK criterion were also compared with those from the above-mentioned eight criteria. It was demonstrated that the SKK criterion not only responds well to all studied process parameters but also rightly predicts the occurrence of hot tears under given casting parameters. Here, combined with experimental data, the SKK criterion is implemented to predict the effect of main alloying elements on the hot tearing susceptibility of grain-refined Al-xZn-yMg-zCu alloys.

II. EXPERIMENT

A. *Alloy Preparation*

Grain-refined Al-xZn-yMg-zCu model alloys with variant Zn (x = 2, 4, 6, 9, and 12 wt pct), Mg (y = 1.5, 2, and 2.5 wt pct), and Cu (z = 1, 1.5, and 2 wt pct) contents were prepared using pure Al (99.99 wt pct), Zn (99.99 wt pct), and Mg (99.9 wt pct) and Al-50 wt pct Cu master alloys. Melting was conducted in a graphite crucible (1 kg capacity) using an electrical resistance furnace under dry (normal atmospheric) conditions. The melt was heated up to 1013 K and held for 5 minutes. Then, 0.4 wt pct Al-5Ti-1B master alloy was added for grain refinement. After stirring for 1 minute, removal of slag, and holding for 15 minutes, the melt was poured into the hot tearing testing apparatus. The actual chemical compositions of the cast alloys are listed in Table I. Note that the chosen compositions are typical for commercial 7xxx alloys.[15] Four commercial 7xxx aluminum alloys were also investigated in the discussion part, and compositions are included in Table I.

B. *Hot Tearing Rating Apparatus*

The apparatus simulating DC-casting conditions of sheet ingots is shown in Figure 1, which consists of the following major parts: a T-shaped graphite mold with a graphite block, a water-cooled bronze base, a load cell, a setup for fastening the load cell, and a data acquisition system. The apparatus is modified based on the linear contraction measurement apparatus.[17] However, replacing the displacement sensor in Reference 17, the load cell and fasten setup are applied to constrain the casting. As shown in Figure 1, when the melt is poured into the middle of the T-shaped mold, the melt solidifies first at the T-shaped end with a thinner cross section and graphite block. The load cell, which is fixed tightly to the base to ensure no movement during solidification, is attached to a metallic screw which is run through the graphite block to measure the tensile load. Thus, the casting is restricted and can induce hot tearing. Note that the negative effect of friction is eliminated by using graphite materials.

As shown in Figure 1, a K-type thermocouple was used to measure the temperature evolution during solidification. The thermocouple was inserted from the mold bottom to minimize its effect on the load data acquisition. Two sets of experiments were performed in this study: with and without the thermocouple. The first

Table I. Actual Chemical Compositions of the Grain-Refined Al-*x*Zn-*y*Mg-*z*Cu Model Alloys and Four Commercial 7xxx Alloys (Wt Percent)

Alloys	Zn	Mg	Cu	Ti	Fe	Si	Mn	Cr	Zr	Al
Al-2Zn-2Mg-2Cu	1.80	1.85	1.90	0.014	0.009	0.011				bal.
Al-4Zn-2Mg-2Cu	3.72	1.94	2.00	0.014	0.010	0.010				bal.
Al-6Zn-2Mg-2Cu	5.57	1.77	2.04	0.014	0.008	0.010				bal.
Al-9Zn-2Mg-2Cu	8.27	1.85	1.94	0.014	0.010	0.015				bal.
Al-12Zn-2Mg-2Cu	11.50	1.94	1.96	0.014	0.008	0.013				bal.
Al-9Zn-1.5Mg-2Cu	8.41	1.41	2.11	0.014	0.009	0.013				bal.
Al-9Zn-2Mg-2Cu	8.63	1.81	1.91	0.014	0.008	0.011				bal.
Al-9Zn-2.5Mg-2Cu	8.55	2.19	2.03	0.014	0.008	0.009				bal.
Al-9Zn-2Mg-1Cu	8.51	2.02	0.91	0.014	0.010	0.008				bal.
Al-9Zn-2Mg-1.5Cu	8.71	1.99	1.45	0.014	0.009	0.015				bal.
AA7022	4.75	3.54	0.75	0.014	0.030	0.021	0.25	0.18	0.02	bal.
AA7050	6.25	2.10	2.10	0.014	0.021	0.018	0.01	0.01	0.10	bal.
AA7085	7.35	1.6	1.64	0.014	0.03	0.03	0.01	0.01	0.09	bal.
AA7055	8.05	2.14	2.01	0.014	0.025	0.020	0.01	0.01	0.14	bal.

one measured the temperature and load evolution simultaneously, while the second one measured the crack width by avoiding cracking initiated by the thermocouple. Different from previous work,[2] ceramic fiber materials with different thicknesses were applied to the center of the T-shaped mold in these two sets of experiments to adjust the severity of hot tearing. Note that the materials used in the first experiment are thinner than those used in the second experiment. The aim of using thinner materials is to prevent the occurrence of hot cracks and to obtain the load development curve without interruptions during solidification. Although the cooling rates in the two experiments are different (about 5 K/s), the obtained load data in the first experiment can be used to explain the measured hot tearing susceptibility in the second experiment. Figure 2(a) shows the cooling curves in the middle and bottom of the center of the T-shaped mold. No obvious difference is observed during the last stage of solidification because of the good thermal insulation of the applied ceramic fiber materials. It implies that the temperature field from bottom to top in the center of the T-shaped mold is approximately uniform. Three castings were repeated at least for each composition. Note that the measured cooling rates during solidification are between 7 and 12 K/s depending on the thickness of the ceramic fiber materials, which is similar to DC-casting practices.[33]

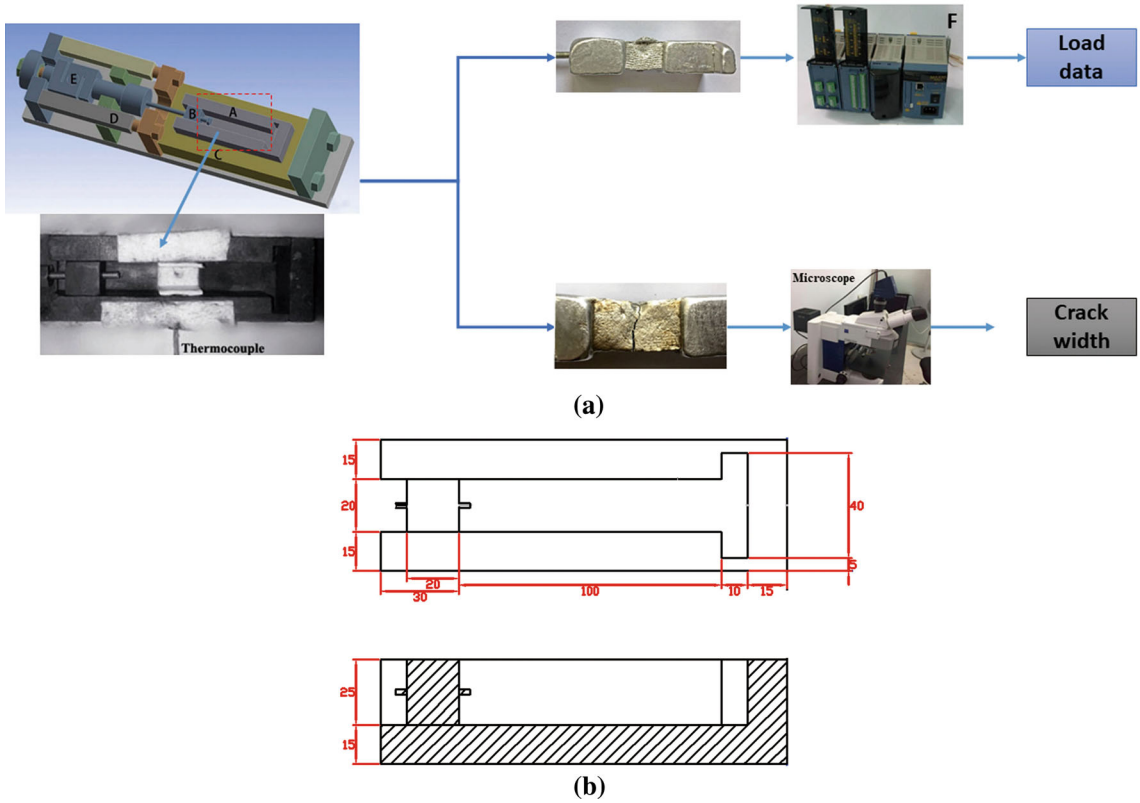

Fig. 1—(*a*) Hot tearing testing apparatus. A: a graphite mold with a T-shaped end; B: a graphite block; C: a water-cooled bronze base; D: a fastener setup; E: a load cell; and F: a data acquisition system; (*b*) dimensional sketch of the T-shaped mold.

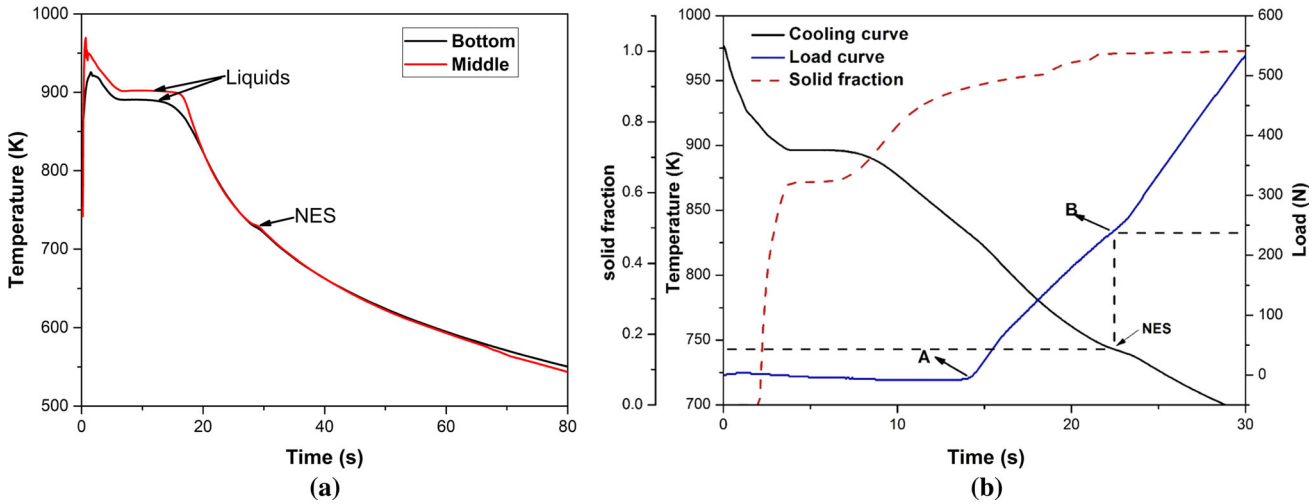

Fig. 2—(*a*) Cooling curves in the middle and bottom of the center of the T-shaped mold; (*b*) temperature, load, and solid fraction as a function of time for grain-refined Al-2Zn-2Mg-2Cu alloy. Point A: load onset. Point B: load at NES.

This apparatus provides much information on the load development during solidification and the size of hot cracks of an alloy. Figure 2 displays an example of the load development curve, and the corresponding cooling and solid fraction curves are also shown. The pre-shrinkage expansion occurs firstly mainly due to the evolution of gas.[17,33] As the solidification proceeds, the dendrites begin to impinge. Strong networks start to form and can transfer tensile loads. Point "A" corresponding to the load onset temperature is regarded as the dendrite rigidity point.[17,21] During the final stage of solidification, the alloy begins to transfer the load more like a solid, due to the formation of solid bridges.[28] When the solidification is completed, point "B" corresponding to non-equilibrium solidus (NES) is obtained. Note that the load

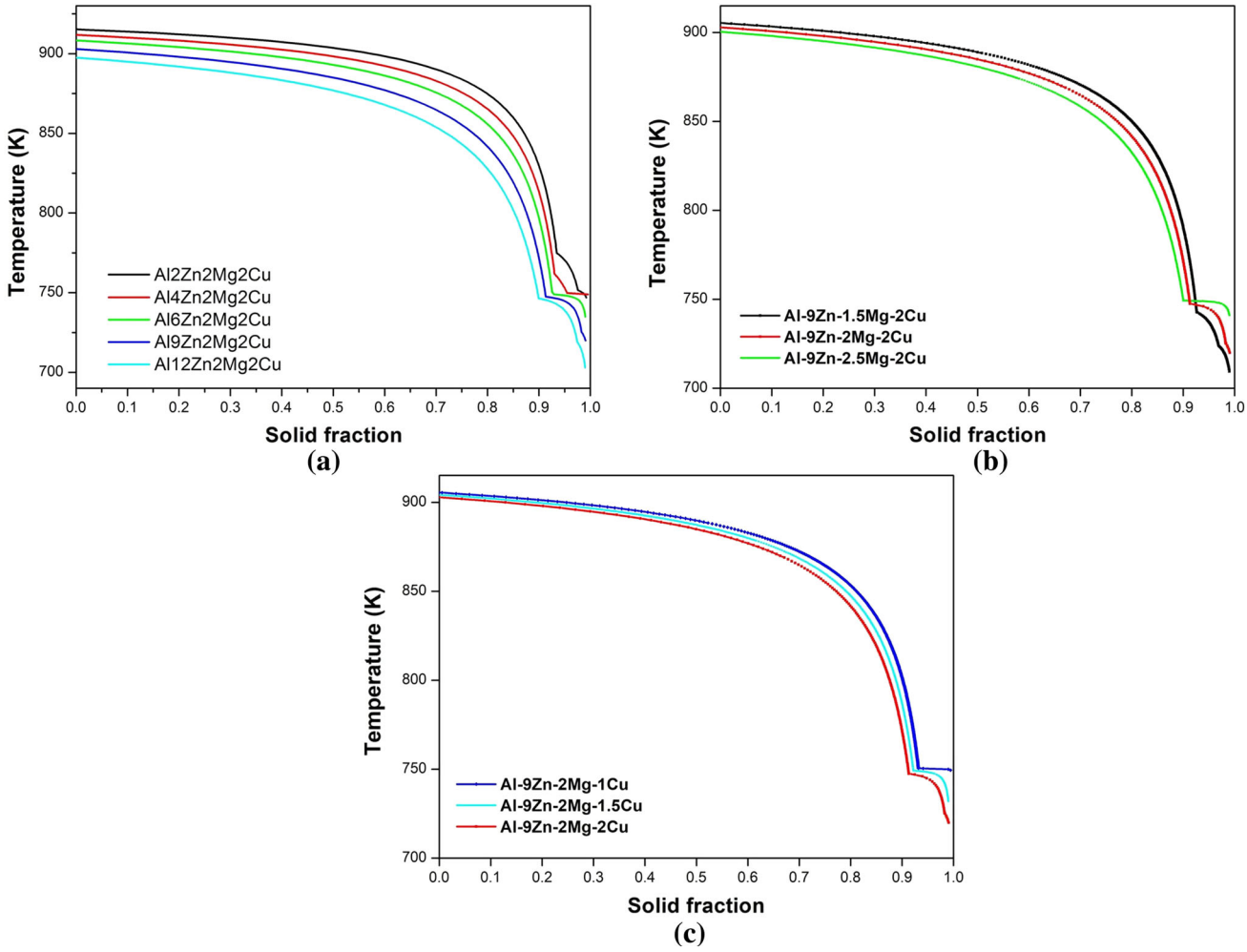

Fig. 3—Temperature of grain-refined (*a*) Al-*x*Zn-2Mg-2Cu, (*b*) Al-9Zn-*y*Mg-2Cu, and (*c*) Al-9Zn-2Mg-*z*Cu alloys plotted as a function of solid fraction (the solidus is taken as 0.99 solid).

Table II. The Solidification Range, Effective Solidification Range Calculated by the Load Onset Temperature and NES, the Amount of Non-equilibrium Eutectics (f_e) of All Studied Alloys Obtained from Thermo-Calc Assuming Scheil–Gulliver Model, and the f_e and Secondary Dendrite Arm Spacing (SDAS) Measured by SEM

Alloy	Solidification Range (K)	Effective Solidification Range (K)	f_e	Measured f_e	SDAS (μm)
Al-2Zn-2Mg-2Cu	168.15	82.45	0.055	0.025 ± 0.005	30 ± 4
Al-4Zn-2Mg-2Cu	163.15	79.15	0.06	0.032 ± 008	25 ± 2
Al-6Zn-2Mg-2Cu	174.15	80.45	0.065	0.039 ± 0.008	27 ± 5
Al-9Zn-2Mg-2Cu	183.15	104.95	0.077	0.042 ± 0.007	21 ± 2
Al-12Zn-2Mg-2Cu	196.15	79.45	0.09	0.043 ± 0.006	14 ± 2
Al-9Zn-1.5Mg-2Cu	196.65	68.1	0.074	0.035 ± 0.01	25 ± 3
Al-9Zn-2Mg-2Cu	183.15	61.75	0.077	0.051 ± 0.007	25 ± 3
Al-9Zn-2.5Mg-2Cu	160.15	27.5	0.09	0.068 ± 0.009	27 ± 3
Al-9Zn-2Mg-1Cu	156.65	18.05	0.062	0.037 ± 0.008	30 ± 5
Al-9Zn-2Mg-1.5Cu	173.15	34.45	0.068	0.063 ± 0.005	24 ± 4
Al-9Zn-2Mg-2Cu	183.15	61.75	0.077	0.051 ± 0.007	25 ± 3

value at NES was found to be a good indicator of the hot tearing susceptibility for grain-refined Al-Cu,[24] grain-refined Al-Mg-Si,[28] non-refined Al-Zn-Mg-Cu[2] alloys, and grain-refined Al-Zn-Mg-Cu alloys, which will be discussed later.

In the second experiment, hot tears formed in the central zone of the T-shaped casting (Figure 1) were observed using an optical microscope, and the maximum crack width was measured. The microstructure of the specimen close to the thermocouple was observed

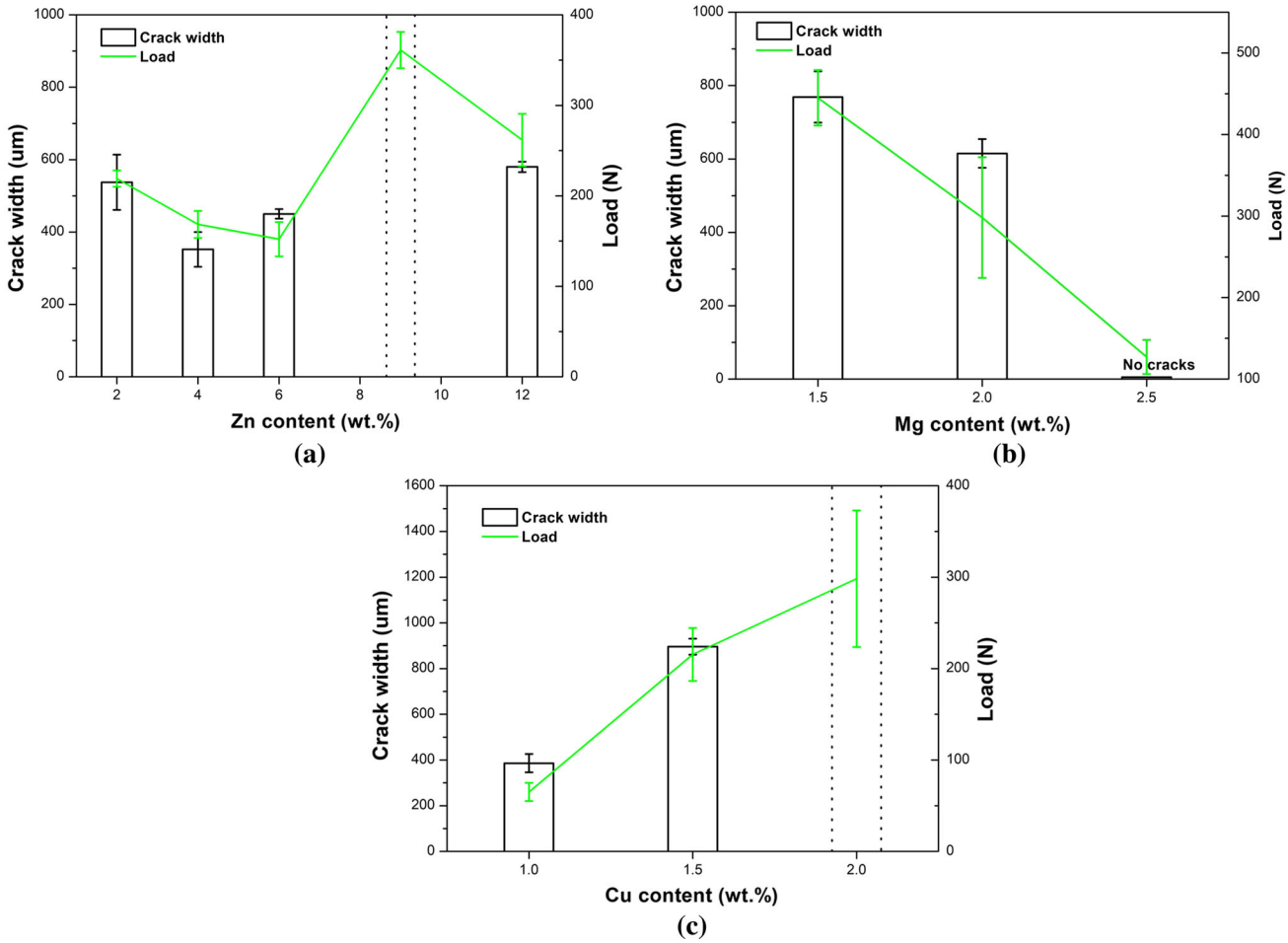

Fig. 4—Variances of maximum crack widths (bar graph) and load values at NES for the refined alloys: (*a*) Al-*x*Zn-2Mg-2Cu, (*b*) Al-9Zn-*y*Mg-2Cu, and (*c*) Al-9Zn-2Mg-*z*Cu alloys. Dashed lines represent that castings are completely fractured. Note that the thickness of the thermal insulation material used in (b) is thinner compared to those in (a) and (c) to avoid complete cracking.

using polarized light in an optical microscope and with a scanning electron microscope (SEM) equipped with an energy-dispersive X-ray spectroscopy module. The grain size was measured using the linear intercept method described in ASTM standard E112-96.

III. RESULTS

A. *Solidification Paths of 7xxx Alloys*

The temperature-solid fraction profiles of all investigated alloys are obtained using Thermo-Calc software assuming Scheil–Gulliver solidification. The results are given in Figure 3 and some key data are listed in Table II. Note that the NES is assumed to correspond to the solid fraction of 0.99, where significant solid bridges have formed and the material behaves like a solid.[2,28] In general, alloying lowers the liquidus and NES temperatures by a few degrees. For grain-refined Al-*x*Zn-2Mg-2Cu alloys, the solidification range firstly decreases from 168.15 to 163.15 K when the Zn content increases from 2 to 4 wt pct, and then rises to 196.15 K at a Zn content of 12 wt pct. The solidification range is decreased by 36.5 K for grain-refined Al-9Zn-*y*Mg-2Cu alloys, when the Mg content goes up from 1.5 to 2.5 wt pct, while the solidification range is increased by 26.5 K with increasing Cu content from 1 to 2 wt pct for grain-refined Al-9Zn-2Mg-*z*Cu alloys. In terms of the amount of non-equilibrium eutectics (Table II), all investigated alloys show an increasing tendency with the addition of alloying elements. Its magnitude gradually increases by 0.035, 0.016, and 0.01 with the increase of Zn, Mg, and Cu contents, respectively. The reliability of the calculations from Thermo-Calc software assuming Scheil–Gulliver solidification will be discussed later.

B. *Influence of Main Alloying Elements*

1. *Crack width measurements*

Firstly, the variance of the maximum crack width of the grain-refined Al-*x*Zn-2Mg-2Cu system is shown in Figure 4(a). Its magnitude firstly decreases from 537.5 μm for Al-2Zn-2Mg-2Cu to the lowest value, *i.e.*, 352 μm, for Al-4Zn-2Mg-2Cu and then slightly returns to 450 μm for Al-6Zn-2Mg-2Cu. The maximum crack width of Al-9Zn-2Mg-2Cu is displayed with

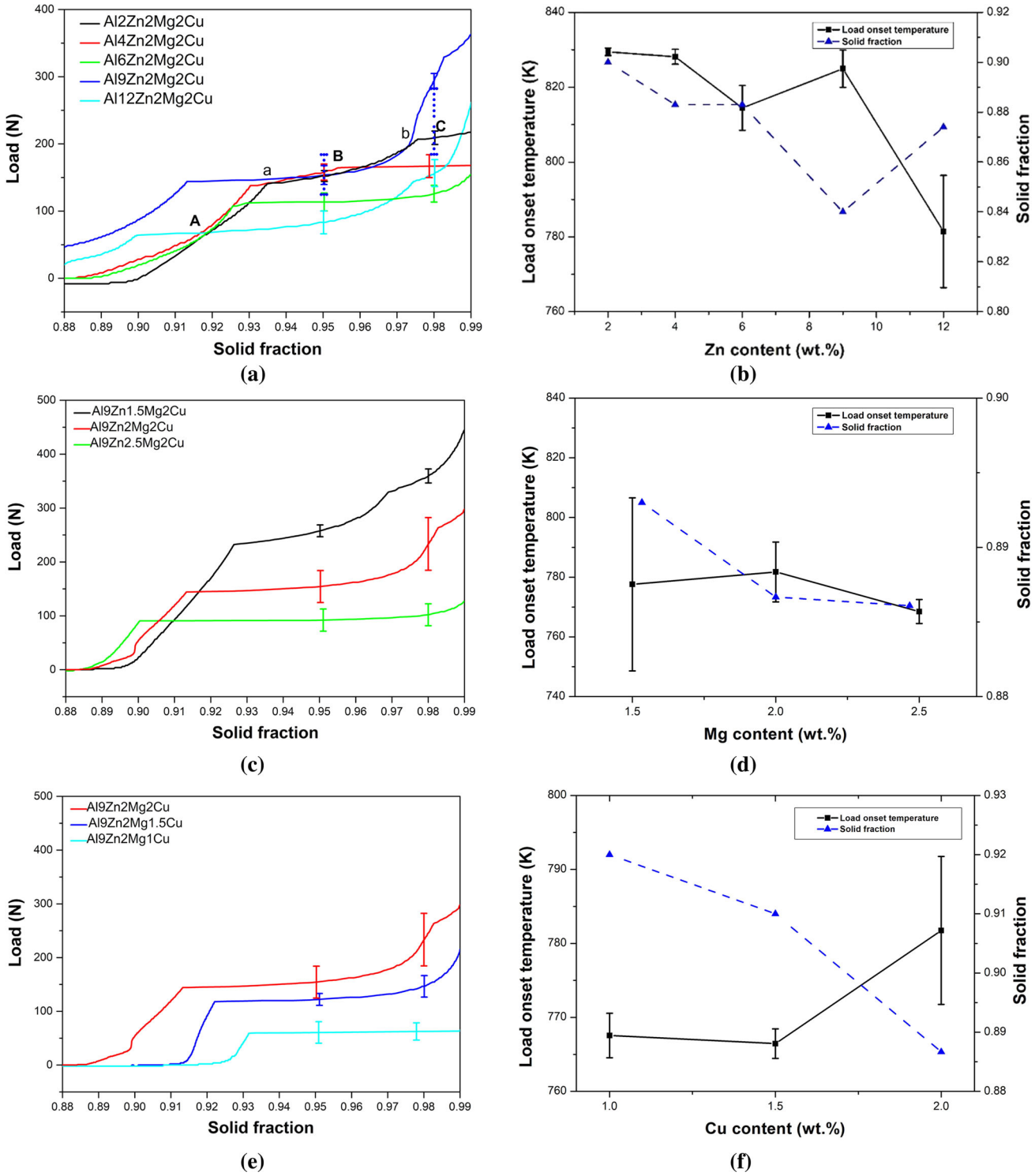

Fig. 5—The load *vs* solid fraction during the last stage of solidification for the grain-refined alloys: (*a*) Al-*x*Zn-2Mg-2Cu alloys, (*c*) Al-9Zn-*y*Mg-2Cu, and (*e*) Al-9Zn-2Mg-*z*Cu alloys. Variances of load onset temperatures and corresponding solid fractions of (*b*) Al-*x*Zn-2Mg-2Cu, (*d*) Al-9Zn-*y*Mg-2Cu, and (*f*) Al-9Zn-2Mg-*z*Cu alloys. Note that the thicknesses of the insulation material used in (c) and (e) are the same but different from that used in (a) to avoid load drop.

dashed lines since the casting was completely cracked, indicating its maximum hot tearing susceptibility. Then, the crack width decreases back to 580 μm for Al-12Zn-2Mg-2Cu.

The variances of the maximum crack width of grain-refined Al-9Zn-*y*Mg-2Cu and Al-9Zn-2Mg-*z*Cu alloys are shown in Figures 4(b) and (c), respectively. For Al-9Zn-*y*Mg-2Cu alloys, the maximum crack width

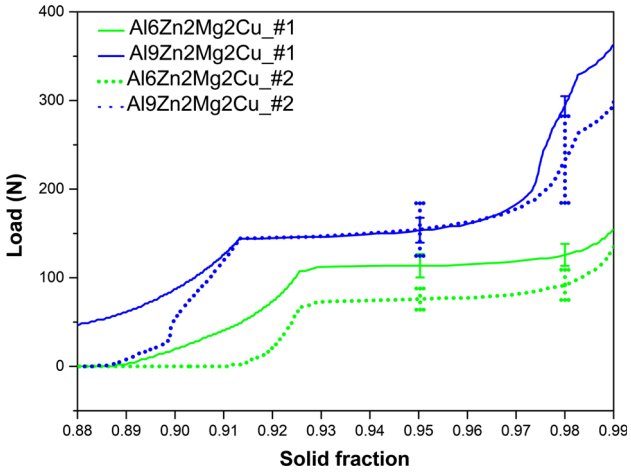

Fig. 6—Comparison of the load development during the last stage of solidification for grain-refined Al-6Zn-2Mg-2Cu and Al-9Zn-2Mg-2Cu alloys under different testing conditions (solid lines represent the testing using thicker materials and dashed lines using thinner materials).

decreases from 769 um to about 600 um with the increase of the Mg content from 1.5 to 2 wt pct. When the Mg content is increased to 2.5 wt pct, no hot tears are observed. Thus, the addition of Mg apparently improves the hot tearing resistance of Al-9Zn-*y*Mg-2Cu alloys. Contrarily, the addition of Cu significantly deteriorates the hot tearing resistance of Al-9Zn-2Mg-*z*Cu alloys. The maximum crack width rises from about 400 μm for the Al-9Zn-2Mg-1Cu alloy to approximately 900 μm for the Al-9Zn-2Mg-1.5Cu alloy. Further increasing the Cu content up to 2 wt pct results in a total fracture.

2. *Load evolution*

The measured load developments as a function of the calculated solid fraction are plotted in Figures 5(a), (c), and (e). Note that the load development actually reflects the tensile stress situation in the hot spot situated in the center of the sample, which will be used as input to the SKK criterion later. Since all these curves show a similar trend, Al-2Zn-2Mg-2Cu alloy is taken as an example. The load curve can be divided into three sections A, B, and C with intersections a and b. Initially, no load response is observed. When the solid fraction corresponding to the load onset temperature, *i.e.*, 0.9, is reached, the load starts to increase rapidly to point a, and then rises gradually to point b. Finally, the load at NES is reached. Note that points a and b correspond to the occurrence of eutectic reactions, which is in accordance with our previous report.[2] Similar load development trends are also observed in other alloys (Figures 5(a), (c), and (e)).

Much information can be obtained from the load development curves shown in Figures 5(a), (c), and (e). Firstly, the load onset temperature and corresponding solid fraction of refined Al-Zn-Mg-Cu alloys are extracted and shown in Figures 5(b), (d), and (f). For Al-*x*Zn-2Mg-2Cu alloys (Figure 5(b)), the solid fraction corresponding to the load onset temperature firstly decreases from 0.9 to 0.84 with increasing Zn content from 2 to 9 wt pct and then goes back to 0.875 when the Zn content is 12 wt pct, whereas the load onset temperature exhibits some fluctuations in the range between 760 and 840 K. For Al-9Zn-*y*Mg-2Cu alloys (Figure 5(d)), the solid fraction corresponding to the load onset temperature shows a slight drop from 0.894 to 0.886 when the Mg content changes from 1.5 to 2 wt pct. Further increase of the Mg content up to 2.5 wt pct has no obvious effect on the solid fraction. For Al-9Zn-2Mg-*z*Cu alloys, the solid fraction corresponding to the load onset temperature decreases from 0.92 at 1 wt pct Cu to 0.886 at 2 wt pct Cu, as shown in Figure 5(f).

In addition, the load values at NES are also obtained from Figures 5(a), (c), and (e) and plotted in Figure 4 for comparison with maximum crack widths. For Al-*x*Zn-2Mg-2Cu alloys, the minimum and maximum load values at NES for the Zn contents are 4 to 6 and 9 wt pct, respectively. Considering the error bars, the load values at NES are in reasonable agreement with the crack widths for Al-*x*Zn-2Mg-2Cu alloys. For Al-9Zn-*y*Mg-2Cu alloys, the load value at NES gradually decreases from 450 N for Al-9Zn-1.5Mg-2Cu to 130 N for Al-9Zn-2.5Mg-2Cu alloy, which is consistent with the variance of the maximum crack width. For Al-9Zn-2Mg-*z*Cu alloys, the load value at NES gradually increases from 60 N for Al-9Zn-2Mg-1Cu to 300 N for Al-9Zn-2Mg-2Cu alloy, which also exhibits the same tendency with the variance of the maximum crack width. Thus, a good correlation between the load value and the hot tearing susceptibility is observed in grain-refined Al-*x*Zn-*y*Mg-*z*Cu alloys.

To investigate the effect of different solidification conditions on load evolutions, measurements with thinner insulation materials were carried out for Al-6Zn-2Mg-2Cu and Al-9Zn-2Mg-2Cu alloys. These results are also compared with those with thicker insulation materials in Figure 5(a), which is shown in Figure 6. Using thinner insulation materials changes the load value at NES and the solid fraction corresponding to the load onset temperature, but their variances are relative. Thus, the measured load developments in the first experiment can be used to reflect the load developments in the second experiment.

3. *Microstructure*

Optical and SEM micrographs of some grain-refined Al-Zn-Mg-Cu alloys are shown in Figure 7. Obviously, all the alloys consist of fine equiaxed grains and the average grain size is almost the same for all the alloys under the same casting conditions (about 55 μm). The addition of alloying elements clearly affects the amount of non-equilibrium eutectics and the value of secondary dendrite arm spacing (SDAS). These values are measured and summarized in Table II. It can be found that the measured amount of eutectics matches well with the calculated values. The value of SDAS decreases with the addition of Zn and Cu. Contrarily, the value of SDAS slightly rises with the addition of Mg. Table III lists the

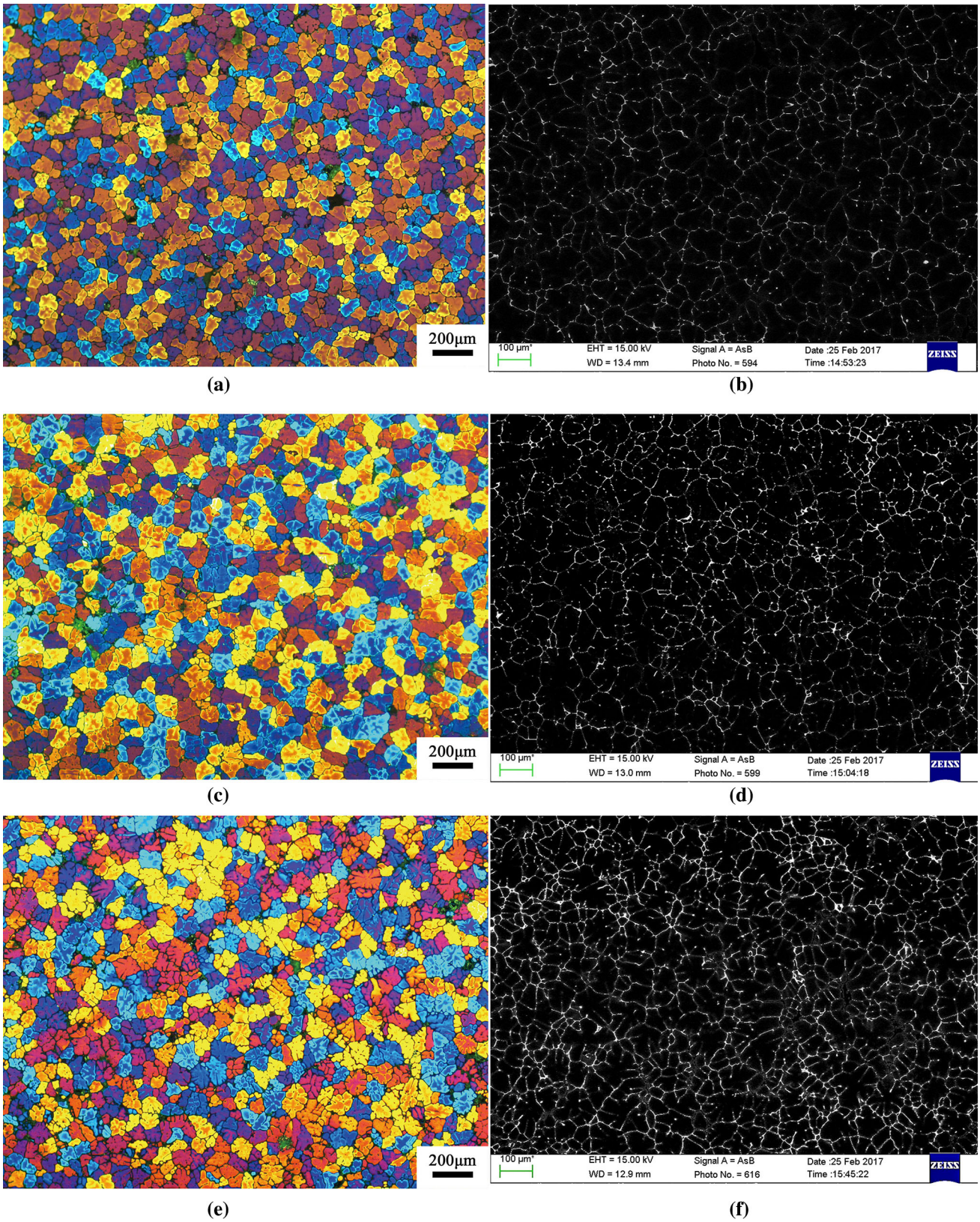

Fig. 7—Optical (*a*, *c*, and *e*) and SEM (*b*, *d*, and *f*) photos in Al-*x*Zn-2Mg-2Cu alloys ($x = 4$ (a, b), 6 (c, d), and 12 (e, f)).

types of non-equilibrium eutectics from SEM observations and Thermo-Calc calculations. Overall, the calculations are in agreement with the observations, which proves the reliability of the calculations, especially for the final eutectics. With increasing Zn content, the Al_2CuMg and AlMgCuZn phases disappear, while more

Table III. Comparison of the Final Eutectics from SEM Observations and Thermo-Calc Calculations

Alloy	SEM Observations	Thermo-Calc Calculations	Differences Between Observations and Calculations
Al-2Zn-2Mg-2Cu	$Al_2CuMg + Al_2Cu + Mg(ZnCuAl)_2 +$ AlMgCuZn	$Al_2CuMg +$ AlMgCuZn + $MgZn_2$	Al_2Cu was observed
Al-4Zn-2Mg-2Cu	$Mg(ZnCuAl)_2$	$Al_2CuMg + MgZn_2$	Al_2CuMg was not observed
Al-6Zn-2Mg-2Cu	$Mg(ZnCuAl)_2 + Al_2Cu$	$Al_2CuMg + MgZn_2$	Al_2Cu was observed, no Al_2CuMg
Al-9Zn-2Mg-2Cu	$Mg(ZnCuAl)_2 + Al_2Cu$	$Al_2Cu + MgZn_2$	
Al-12Zn-2Mg-2Cu	$Mg(ZnCuAl)_2 + Al_2Cu$	$Al_2Cu + MgZn_2$	
Al-9Zn-1.5Mg-2Cu	$Mg(ZnCuAl)_2 + Al_2Cu$	$Al_2Cu + MgZn_2$	
Al-9Zn-2.5Mg-2Cu	$Mg(ZnCuAl)_2$	$MgZn_2$	
Al-9Zn-2Mg-1Cu	$Mg(ZnCuAl)_2$	$MgZn_2$	
Al-9Zn-2Mg-1.5Cu	$Mg(ZnCuAl)_2$	$MgZn_2$	

Note that $MgZn_2$ phase also contains Al and Cu.[5]

$Mg(ZnCuAl)_2$ and Al_2Cu phases precipitate because the $Mg(ZnCuAl)_2$ phase contains more Mg and Cu. Similarly, with increasing Mg content, the formation of $Mg(ZnCuAl)_2$ phase requires more Cu. Thus, the Al_2Cu phase gradually disappears. However, the addition of Cu promotes the precipitation of the Al_2Cu phase.

C. *Hot Tearing Predictions by the SKK Criterion*

In the SKK criterion,[31] three possible phenomena may happen during the last stage of solidification. Firstly, the liquid flow can adequately compensate for the solidification shrinkage and thermal contraction, and therefore no cavities are formed. Secondly, when the feeding ability of the semi-solid becomes limited, micro-pores may form, which depends on the interaction between the shrinkage/contraction and feeding terms. The shrinkage/contraction rate *fr* is given as

$$fr = -\left(\frac{\rho_s}{\rho_l} - 1\right)\frac{\partial f_l}{\partial t} + \left(\frac{\rho_s}{\rho_l}\right)\dot{\varepsilon}, \qquad [1]$$

where ρ_s and ρ_l are the solid and liquid densities, respectively; f_l is the liquid fraction; t is the time; $\dot{\varepsilon}$ is the strain rate. The feeding rate *fe* is expressed as

$$fe = K\frac{P}{\eta L^2} \qquad [2]$$

$$K = \frac{\lambda^2(1-f_s)^3}{180f_s^2} \qquad [3]$$

$$P = P_a + P_m - \frac{4\gamma_{sl}}{\lambda}, \qquad [4]$$

where K is the permeability; P is the feeding pressure; η is the viscosity of liquid; L is the mushy zone length; λ is the SDAS; f_s is the solid fraction; P_a and P_m are the atmospheric pressure and metallostatic pressure, respectively; γ_{sl} is the solid–liquid interfacial energy. The cavity fraction f_v can be expressed by

$$-\frac{\rho_s}{\rho_l}\frac{\partial f_v}{\partial_T}\dot{T} = \left(\frac{\rho_s}{\rho_l} - 1\right)\frac{\partial f_l}{\partial_T}\dot{T} + \left(\frac{\rho_s}{\rho_l}\right)\dot{\varepsilon} - fe \qquad [5]$$

$$f_v = \int_{T_{crit}}^{T} \frac{\partial f_v}{\partial_T}\mathrm{d}T, \qquad [6]$$

where $\dot{T}$ is the cooling rate. T_{crit} is the critical temperature where the feeding rate *fe* is equal to the shrinkage/contraction rate *fr*. Thus, the cavity size d is given as

$$d = \left(\frac{3c}{2\pi}f_v d_g^3\right)^{1/3}, \qquad [7]$$

where c is chosen as $2\sqrt{2}$ for aluminum alloys; d_g is the grain size.

Thirdly, when the cavity size d exceeds a critical size a_{crit}, hot tearing will occur. The a_{crit} is determined by using the Griffith criterion:

$$a_{crit} = 4\gamma_l \frac{E}{\pi\sigma^2}, \quad [8]$$

Table IV. Parameters Used for the SKK Criterion

Parameter	Value	Unit	References
ρ_s	2740	kg/m^3	7
ρ_l	2500	kg/m^3	7
P_a	101	kPa	7
P_m	5000	kPa	2
d_g	96	μm	—
γ_{sl}	0.095	J/m^2	7
γ_l	0.74	J/m^2	7
$\dot{\varepsilon}$	2.25×10^{-4}	s^{-1}	12,40
η	0.0013	Pa s	31
c	$2\sqrt{2}$	—	31
E	170	MPa	—

where γ_l is the surface energy of the liquid phase; E is the Young's modulus of the semi-solid; σ the tensile stress which is derived by the measured load development in Figure 5.

The hot tearing susceptibility (HTS) is defined as

$$\text{HTS} = \frac{d}{a_{crit}}. \quad [9]$$

When HTS > 1, hot tearing will occur. Otherwise, only micro-pores will form. The parameters used in the criterion are summarized in Table IV. Note that the viscosity η, varying with alloy compositions and temperature,[34] is difficult to be determined. In this study, a constant value is chosen for all alloys. And a grain size of 96 μm is used, which is the approximate grain diameter calculated using the method described by Greer *et al.*[35] for the linear intercept value of 55 μm measured in these alloys. The length of mushy zone L is determined by the dendritic rigidity temperature and solvus assuming the thermal gradient being equal to 7500 K/m.[2] Moreover, it is difficult to measure the Young's modulus of the semi-solid materials,[31] and

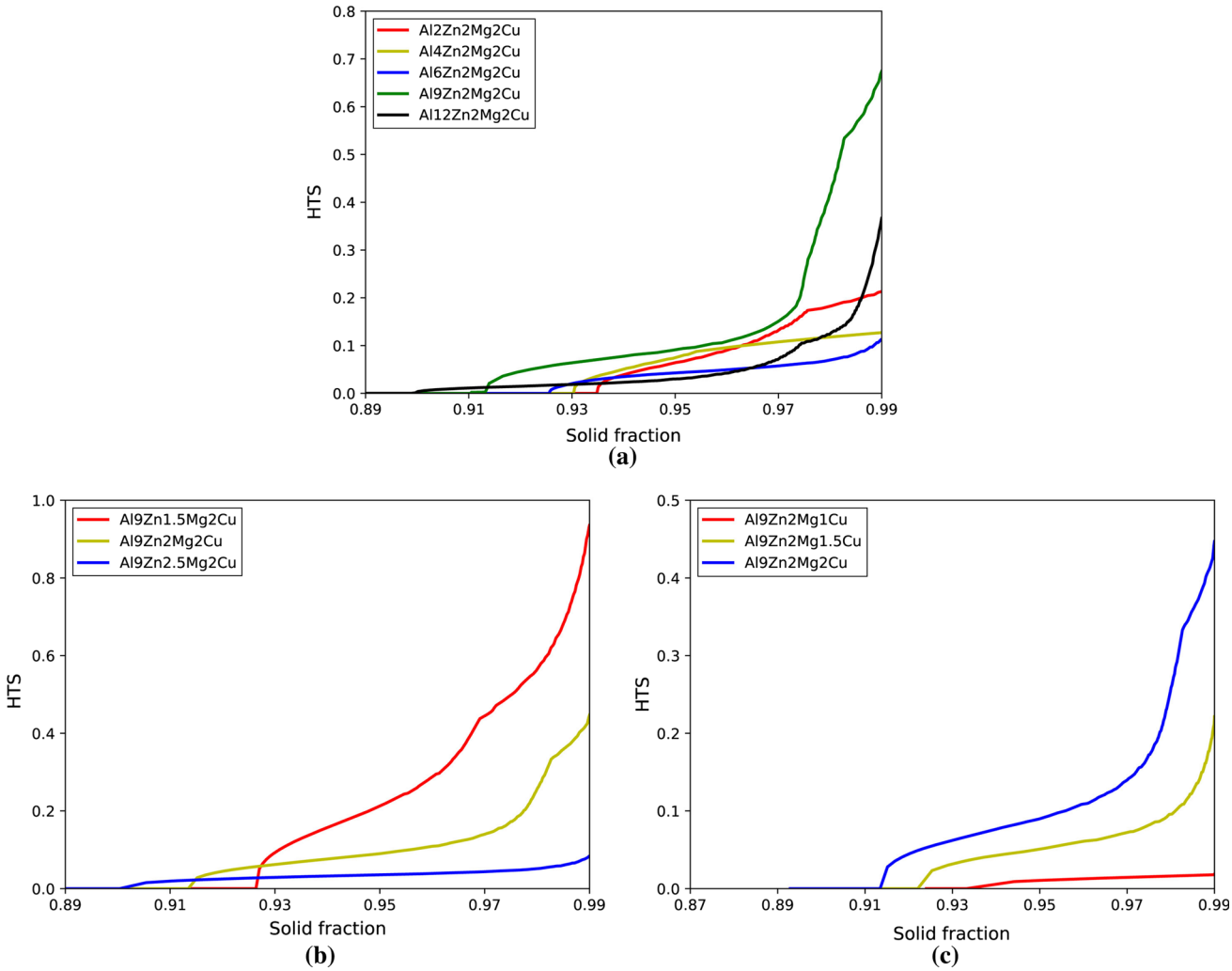

Fig. 8—The predicted HTS by the SKK criterion for (*a*) Al-*x*Zn-2Mg-2Cu, (*b*) Al-9Zn-*y*Mg-2Cu, and (*c*) Al-9Zn-2Mg-*z*Cu alloys.

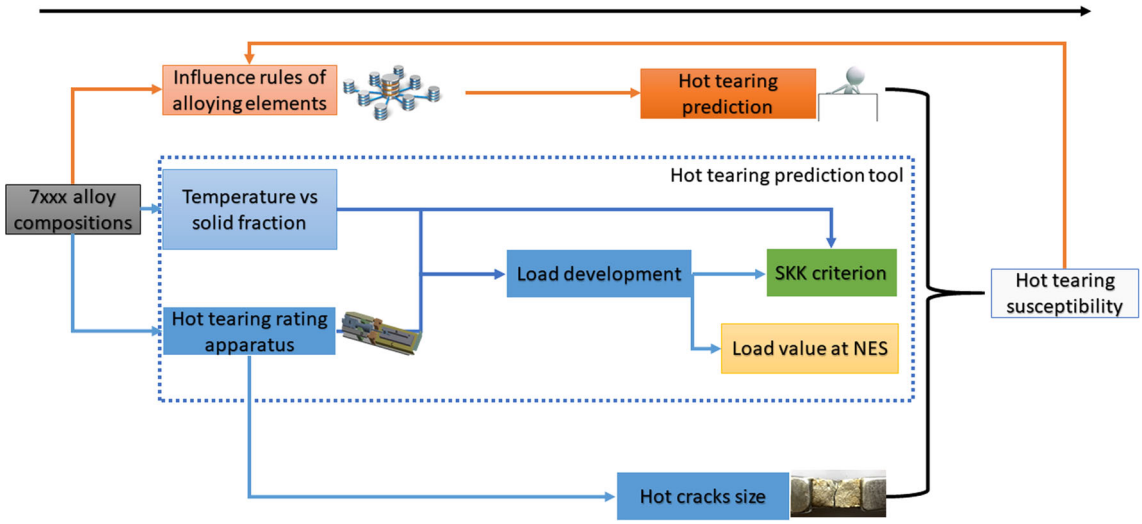

Fig. 9—An outline of the hot tearing evaluation method for DC-casting 7xxx alloys.

here 170 MPa is chosen which lies between those used by Suyitno *et al.*[16] and Bai *et al.*[7]

Figure 8 gives the results predicted by the SKK criterion. For all compositions, the HTS increases with the increase of solid fraction. For Al-*x*Zn-2Mg-2Cu alloys, the predicted maximum and minimum values of HTS in the solid fraction of 0.99 occur at Zn contents of 9 and 4 to 6 wt pct, respectively. The predicted HTS in the solid fraction of 0.99 decreases with the addition of Mg content, while the predicted value increases with the addition of Cu. All of these variances are in agreement with the variances of crack widths and load at NES shown in Figure 4. Furthermore, all predicted values are less than one, indicating no hot tears are formed for all investigated alloys. This is also consistent with the experimental results.

IV. DISCUSSION

In this study, a combined experimental and theoretical approach is implemented to investigate the influence of main alloying elements on the hot tearing susceptibility of grain-refined Al-*x*Zn-*y*Mg-*z*Cu alloys. An outline of this approach is given in Figure 9. The experimental apparatus provides the size of hot tears and information on the load developments during solidification which is further used as input to the SKK criterion to predict the hot tearing susceptibility. The predictions are in agreement with the experimental measurements. In addition, the load values at NES are also found to be a good indicator for hot tearing occurrence.

Using this method, the effects of the main alloying elements are obtained. The effect of Zn is more complicated for grain-refined Al-*x*Zn-2Mg-2Cu alloys and the minimum and maximum hot tearing susceptibilities occur for 4 to 6 and 9 wt pct Zn, respectively. The increase of Mg has a positive effect on improving the hot tearing resistance of grain-refined Al-9Zn-*y*Mg-2Cu alloys, while the increase of Cu has a negative effect on the hot tearing resistance of grain-refined Al-9Zn-2Mg-*z*Cu alloys. These tendencies are attributed to the interplay between thermal stresses and melt feeding. The SKK criterion considers these factors and correctly predicts the tendencies of the main alloying elements, as shown in Figure 8.

The thermal stress represented by the load at NES is a good indicator of the hot tearing susceptibility (Figure 4), which was also observed in References 2, 24, and 28. According to Eq. [8], the higher the load at NES is, the smaller the critical size a_{crit} at NES is. Thus, a hot tear is more likely to be formed. It should be pointed out that the hot tearing susceptibility also depends on the cavity size d according to Eq. [9]. However, a contrary relationship was reported in non-refined Al-Cu[19] and Al-0.52Mg-0.34Si-xFe alloys.[29] For the former, this may be because the occurrence of hot tears releases more load in non-refined Al-Cu alloys, which has been pointed out in our previous work.[2] For the latter, a three-dimensional network of Fe-based intermetallics has formed at higher Fe contents, which promotes the earlier formation of solid bridges and thus leads to a higher load value at NES and lower hot tearing susceptibility.[29] Note that there are still no industrial scale data available to check the relationship between the load at NES and the hot tearing susceptibility.

Additionally, the solidification path, especially the final eutectics, which is the key input of the alloy composition into the SKK model, is closely related to the hot tearing susceptibility. Interestingly by comparing the hot tearing susceptibility (Figure 4) with the final eutectics (Table III), the low-melting Al_2Cu phase does not occur in the alloy with the low hot tearing susceptibility, such as Al-4Zn-2Mg-2Cu, Al-9Zn-2.5Mg-2Cu, and Al-9Zn-2Mg-1Cu alloys. Thus, it is thought that the occurrence of the low-melting Al_2Cu phase will harm the hot tearing resistance of Al-Zn-Mg-Cu alloys.

The authors previously[2] suggested that an inverted lambda curve for non-grain-refined Al-*x*Zn-2Mg-2Cu alloys is obtained where the minimum and maximum crack widths occur at 4 and 12 wt pct Zn contents, respectively. When grain refiners are added, as shown in Figure 4, the Zn content corresponding to the minimum crack width is almost kept invariant, but the content corresponding to the maximum crack width is shifted from 12 to 9 wt pct. This can be explained by the load development and melt feeding ability. Firstly, by comparing the load developments of non-grain-refined (Figure 10 in Ref. 2) and grain-refined Al-9Zn-2Mg-2Cu and Al-12Zn-2Mg-2Cu alloys (Figure 5(a)), it can be observed that grain refinement delays the load onset point, and therefore the load development of grain-refined Al-12Zn-2Mg-2Cu does not exceed that of grain-refined Al-9Zn-2Mg-2Cu during the last solidification stage, which is different from that occurred in non-grain-refined alloys. Thus, grain-refined Al-12Zn-2Mg-2Cu is subjected to lower tensile stresses than grain-refined Al-9Zn-2Mg-2Cu, resulting in the lower hot tearing susceptibility. Actually, grain refinement often delays the load onset point and thus the load development during solidification due to the finer and more equiaxed grain structure.[12,36] Moreover, the feeding ability is also important and it can be reflected by the amount of non-equilibrium eutectics (Table II). Grain-refined Al-12Zn-2Mg-2Cu has more non-equilibrium eutectics than grain-refined Al-9Zn-2Mg-2Cu, indicating a better feeding ability. Grain-refined Al-12Zn-2Mg-2Cu is subjected to lower tensile stresses and has a better liquid feeding ability, and therefore exhibits a lower hot tearing susceptibility than grain-refined Al-9Zn-2Mg-2Cu. This suggests that higher Zn contents could improve the hot tearing resistance of 7xxx alloys, which is consistent with the industrial experience of the Aluminum Corporation of China that some 7xxx alloys with high Zn contents are not too difficult to be fabricated.

The model alloys, *i.e.*, grain-refined Al-Zn-Mg-Cu alloys, are the base of commercial 7xxx alloys, so the effects of alloying elements on the hot tearing susceptibility can be easily applied to 7xxx alloys. This is verified below by comparing the compositions of four common commercial 7xxx alloys (Table I) with their hot tearing susceptibilities indicted by the amount of linear contraction. A previous report[17] has suggested that the linear contraction during solidification can successfully reflect the hot tearing susceptibility. The rating of the amount of linear contraction for the four alloys is given as AA7022 < AA7050 < AA7085 < AA7055.[10] Here, this linear contraction is compared with the hot tearing predictions below. Compared with other alloys, AA7022 has the lowest Cu content and the highest Mg content, and its Zn content is closer to 4 to 6 wt pct. According to the influence of the main elements (Figure 4), these compositions lead to the lowest hot tearing susceptibility among these 7xxx alloys. Furthermore, the two alloys, *i.e.*, AA7050 and AA7055, have similar compositions except for the Zn content. AA7055 is much more prone to hot cracking due to its Zn content being closer to 9 wt pct (Figure 4). AA7085 has moderate Zn content, lower Mg and Cu content, which makes its hot tearing susceptibility lie between AA7055 and AA7050. Hence, the effects of alloying elements attained in this study can be used as a guideline to evaluate the hot tearing susceptibility for new 7xxx alloy beforehand, as shown in Figure 9.

In this study, the SKK criterion not only successfully predicts the hot tearing tendencies but also whether hot tears will be formed. The measured tensile stress development is used as input to the SKK criterion to predict the effect of compositions on the hot tearing susceptibility in DC-casting 7xxx alloys. It is proposed to employ this criterion to more commercial 7xxx aluminum alloys. However, it is hard to obtain critical parameters, *i.e.*, Young's modulus, due to the low strength and ductility of the semi-solid materials. Its variance will obviously affect the predictions.[7,16] Also, the viscosity is needed to be determined for every composition. Thirdly, the SKK criterion always predicts an increasing hot tearing tendency during solidification, which does not agree with the casting practice. This is attributed to the assumption that all grains are surrounded by the liquid film during the entire solidification. However, it is known that certain grain bridging occurs during the last stage of solidification.[37–39] Recently, Bai *et al.*[7] improved this criterion by considering the effect of solid bridging/grain coalescence, which plays an important role in hot tearing. Two important parameters were introduced into the criterion, including the fraction of grain boundaries covered by liquid and a solid energy term, representing the energy for hot tear propagation along coalesced grain boundaries. Currently, no data are available on the fraction of grain boundaries covered by the liquid for the studied compositions. In future, the effect of solid bridges should also be included by applying the modified SKK criterion.[7] Finally, the effect of minor elements (Fe and Si) on the hot tearing susceptibility of 7xxx alloys requires further investigations.

V. CONCLUSIONS

The effect of main alloying elements on hot tearing of 7xxx model alloys was investigated by hot tear observations, load measurements, solidification path calculations, and predictions using the SKK criteria. The main conclusions are listed below:

1. The minimum and maximum hot tearing susceptibilities of grain-refined Al-*x*Zn-2Mg-2Cu alloys are observed at Zn contents of 4 to 6 and 9 wt pct, respectively. This hot tearing tendency is different from that observed in non-refined Al-*x*Zn-2Mg-2Cu alloys. The addition of Mg lowers the hot tearing susceptibility of grain-refined Al-9Zn-*y*Mg-2Cu alloys, while the addition of Cu promotes the hot tearing susceptibility of Al-9Zn-2Mg-*z*Cu alloys. This is attributed to the interaction of the tensile stresses, melt feeding, and final eutectics.

2. The effects of alloying elements on the hot tearing susceptibility can be regarded as guidelines and were successfully applied to four commercial 7xxx alloys.
3. The load value at NES is found to be a good indicator for predicting the hot tearing susceptibility in the studied 7xxx alloys. The SKK criterion combined with the measured load developments not only successfully predicts the hot tearing tendencies of these 7xxx alloys but also accurately indicates whether hot tears will occur.

ACKNOWLEDGMENTS

This study was supported by the Major State Research and Development Program of China (Grant No. 2016YFB0300801); the National Natural Science Foundation of China (Grant No. 51671017); the Beijing Laboratory of Metallic Materials and Processing for Modern Transportation; and the Fundamental Research Funds for the Central Universities (Grant No. FRF-GF-17-B3). The authors would like to thank Dr. Q. Du from SINTEF for a valuable discussion.

CONFLICT OF INTEREST

The authors declare that they have no competing interests.

REFERENCES

1. J. Shin, T. Kim, D. Kim, D. Kim, and K. Kim: *J. Alloys Compd.*, 2017, vol. 698, pp. 577–90.
2. Y. Li, X. Gao, Z.R. Zhang, W.L. Xiao, H.X. Li, Q. Du, L. Katgerman, J.S. Zhang, and L.Z. Zhuang: *Metall. Mater. Trans. A*, 2017, vol. 48A, pp. 4744–54.
3. H. Zhao, F. De Geuser, A. Kwiatkowski da Silva, A. Szczepaniak, B. Gault, D. Ponge, and D. Raabe: *Acta Mater.*, 2018, vol. 156, pp. 318–29.
4. D. Gildemeister: *Effects of Microstructure on Hot Cracking Behavior in Al-Zn-Mg-Cu Alloys. TMS Annual Meeting & Exhibition*, Springer, Cham, 2018, pp. 1097–1104.
5. K. Ellingsen, Q. Du, M. M'Hamdi, B.E. Gihleengen, R. Ledal, K.O. Tveito, and A. Håkonsen: *Experimental Study and Numerical Analysis of Cracking During DC Casting of Large Dimension 7075 Aluminium Billets. TMS Annual Meeting & Exhibition*, Springer, Cham, 2018, pp. 895–900.
6. J. Zuo, L. Hou, J. Shi, H. Cui, L. Zhuang, and J. Zhang: *J. Alloys Compd.*, 2017, vol. 708, pp. 1131–40.
7. Q.L. Bai, J.C. Liu, H.X. Li, Q. Du, L. Katgerman, J.S. Zhang, and L.Z. Zhuang: *Mater. Sci. Technol.*, 2016, vol. 32, pp. 846–54.
8. D.G. Eskin: *Physical Metallurgy of Direct Chill Casting of Aluminum Alloys*, CRC Press, Boca Raton, 2008.
9. S. Benum, D. Mortensen, H. Fjær, H.-G. Øverlie, and O. Reiso: On the Mechanism of Surface Cracking in DC Cast 7XXX and 6XXX Extrusion Ingot Alloys in *Essential Readings in Light Metals: Volume 3 Cast Shop for Aluminum Production*, J.F. Grandfield and D.G. Eskin, eds., Springer, Cham, 2016, pp. 887–94.
10. Q.L. Bai, J.C. Liu, Y. Li, H.X. Li, Q. Du, J.S. Zhang, and L.Z. Zhuang: *Mater. Sci. Forum*, 2015, vol. 28, pp. 21–26.
11. Q.L. Bai, Y. Li, H.X. Li, Q. Du, J.S. Zhang, and L.Z. Zhuang: *Metall. Mater. Trans. A*, 2016, vol. 47A, pp. 4080–91.
12. Y. Li, Q. Bai, J. Liu, H. Li, Q. Du, J. Zhang, and L. Zhuang: *Metall. Mater. Trans. A*, 2016, vol. 47A, pp. 4024–37.
13. D. Warrington and D.G. McCartney: *Cast Met.*, 1991, vol. 3, pp. 202–08.
14. D.G. Eskin, S. Suyitno, and L. Katgerman: *Prog. Mater. Sci.*, 2004, vol. 49, pp. 629–711.
15. Aluminum Association: *International Alloy Designations and Chemical Composition Limits for Wrought Aluminum and Wrought Aluminum Alloys*, Aluminum Association, Arlington, 2009.
16. S. Suyitno, W. Kool, and L. Katgerman: *Metall. Mater. Trans. A*, 2005, vol. 36A, pp. 1537–46.
17. D.G. Eskin, S. Suyitno, J.F. Mooney, and L. Katgerman: *Metall. Mater. Trans. A*, 2004, vol. 35A, pp. 1325–35.
18. Z. Wang, Y. Huang, A. Srinivasan, Z. Liu, F. Beckmann, K.U. Kainer, and N. Hort: *Mater. Des.*, 2013, vol. 47, pp. 90–100.
19. S. Li, K. Sadayappan, and D. Apelian: *Metall. Mater. Trans. B*, 2013, vol. 44B, pp. 614–23.
20. G. Cao, I. Haygood, and S. Kou: *Metall. Mater. Trans. A*, 2010, vol. 41A, pp. 2139–50.
21. J.-M. Drezet, B. Mireux, G. Kurtuldu, O. Magdysyuk, and M. Drakopoulos: *Metall. Mater. Trans. A*, 2015, vol. 46A, pp. 4183–90.
22. S. Instone, D. St John, and J. Grandfield: *Int. J. Cast Met. Res.*, 2000, vol. 12, pp. 441–56.
23. M. Pekguleryuz, X. Li, and C. Aliravci: *Metall. Mater. Trans. A*, 2009, vol. 40A, pp. 1436–56.
24. A. Stangeland, A. Mo, M. M'Hamdi, D. Viano, and C. Davidson: *Metall. Mater. Trans. A*, 2006, vol. 37A, pp. 705–14.
25. D. Viano, D. StJohn, J. Grandfield, and C. Cáceres: *Hot Tearing in Aluminium-Copper Alloys*, Springer, Cham, 2016.
26. J. Mitchell, S. Cockcroft, D. Viano, C. Davidson, and D. StJohn: *Metall. Mater. Trans. A*, 2007, vol. 38A, pp. 2503–12.
27. L. Sweet, J. Taylor, M. Easton, M. Couper, and N. Parson: *Chemical Additions to Reduce Hot Tearing in the Cast House, Light Metals 2012*, Springer, Cham, 2012, pp. 1133–38.
28. M.A. Easton, H. Wang, J. Grandfield, C.J. Davidson, D.H. StJohn, L.D. Sweet, and M.J. Couper: *Metall. Mater. Trans. A*, 2012, vol. 43A, pp. 3227–38.
29. L. Sweet, M.A. Easton, J.A. Taylor, J.F. Grandfield, C.J. Davidson, L. Lu, M.J. Couper, and D.H. StJohn: *Metall. Mater. Trans. A*, 2013, vol. 44A, pp. 5396–5407.
30. M. M'Hamdi, A. Mo, and H.G. Fjær: *Metall. Mater. Trans. A*, 2006, vol. 37A, pp. 3069–83.
31. S. Suyitno, W. Kool, and L. Katgerman: *Metall. Mater. Trans. A*, 2009, vol. 40A, pp. 2388–2400.
32. M. Rappaz, J.-M. Drezet, and M. Gremaud: *Metall. Mater. Trans. A*, 1999, vol. 30A, pp. 449–55.
33. L. Zhang, D.G. Eskin, M. Lalpoor, and L. Katgerman: *Mater. Sci. Eng. A*, 2010, vol. 527, pp. 3264–70.
34. A. Dinsdale and P. Quested: *J. Mater. Sci.*, 2004, vol. 39, pp. 7221–28.
35. A.L. Greer, A.M. Bunn, A. Tronche, P.V. Evans, and D.J. Bristow: *Acta Mater.*, 2000, vol. 48, pp. 2823–35.
36. M. Easton, H. Wang, J. Grandfield, D. St John, and E. Sweet: *Mater. Forum*, 2004, vol. 28, pp. 224–29.
37. S. Vernède, J.A. Dantzig, and M. Rappaz: *Acta Mater.*, 2009, vol. 57, pp. 1554–69.
38. M. Sistaninia, S. Terzi, A.B. Phillion, J.M. Drezet, and M. Rappaz: *Acta Mater.*, 2013, vol. 61, pp. 3831–41.
39. S. Geng, P. Jiang, X. Shao, G. Mi, H. Wu, Y. Ai, C. Wang, C. Han, R. Chen, W. Liu, and Y. Zhang: *Acta Mater.*, 2018, vol. 160, pp. 85–96.
40. J.F. Grandfield, C.J. Davidson, and J.A. Taylor: *Contin. Cast.*, 2000, vol. 24, pp. 205–10.